forests

Article

Responses of Stream Water Temperature to Water Levels in Forested Catchments of South Korea

Sooyoun Nam, Honggeun Lim, Byoungki Choi, Qiwen Li, Haewon Moon and Hyung Tae Choi *

Forest Environment and Conservation Department, National Institute of Forest Science, Seoul 02455, Republic of Korea; sysayks87@korea.kr (S.N.); hgh3514@korea.kr (H.L.); vegetation01@korea.kr (B.C.); gimunlee2@korea.kr (Q.L.); haewonii@korea.kr (H.M.)
* Correspondence: choiht@korea.kr; Tel.: +82-2-961-2641

Abstract: Event flow characteristics were evaluated based on temperature and level of stream water in 22 forested catchments (area: 13.2–281.4 ha) to investigate sustainable flood management measures. Temperature and stream water levels were during 346 rainfall events in the summer season (July–September) from 2020 to 2022. Rising stream water levels responded to falling stream water temperature between ≤100 and >100 ha forested catchments in two types of time of concentration. Stream water temperature decreased by 3.0 °C when the stream water level increased by up to 0.9 m during rainfall events. Falling stream water temperature at two types of time of concentration was negatively correlated with total precipitation and rising stream water level. Based on the relatively high value of regression and cumulative frequency distribution, the estimated rising stream water level was appropriate in small catchments (≤100 ha) when the stream water temperature decreased, and the stream water level increased during rainfall events. Rising stream water levels and falling stream water temperatures are responses to catchment-scale effects, which are influenced by the nature and rapidity of the hydrological responses. Therefore, the results of the present study indicate that spatial and temporal differences in thermal responses of stream water temperature to water levels were controlled by catchment-scale effects under rapidly changing rainfall.

Keywords: stream water temperature changes; event water level; forested areas; catchment-scale; event-driven indicator

check for updates

Citation: Nam, S.; Lim, H.; Choi, B.; Li, Q.; Moon, H.; Choi, H.T. Responses of Stream Water Temperature to Water Levels in Forested Catchments of South Korea. *Forests* **2023**, *14*, 2085. https://doi.org/10.3390/f14102085

Academic Editors: Liangxin Fan, Xiaohu Dang and Lie Xiao

Received: 20 September 2023
Revised: 13 October 2023
Accepted: 16 October 2023
Published: 18 October 2023

1. Introduction

The average global temperature is currently rising owing to climate change events [1,2]. IPCC [3] reported that the global average surface air temperature increased by 0.85 °C between 1880 and 2012, whereas the rate of increase has been much higher since 1971 (0.2 °C/decade). Rising temperatures have increased the frequency and intensity of extreme weather events [4,5]. Wu et al. [6] explained that extreme weather events, which usually have a frequency of less than 5%, will become more recurrent due to climate change. Consequently, such events are likely to affect water demand planning and lead to changes in precipitation and runoff patterns because of imbalances in the supply and demand of water resources and their management [7–9].

In the Republic of Korea, 63% of the land is covered by forests, and streams (i.e., tertiary streams) account for 88.9% of the total length of streams nationally [10,11]. Therefore, the streams play a significant role in water supply and management [12]. However, the streams located in the upper parts of catchments have relatively low flow rates, with ephemeral streams, when compared with rivers and lakes located in the lower part of the catchment [13,14]. Therefore, the streams can occur quickly in response to the start of rainfall events [15]. Moreover, variation in discharge in drainages smaller than 100 ha is greater than that in drainages larger than 100 ha, based on the representative elementary area concept [16,17]. For instance, previous studies [16,18] have noted that hydrological processes within 100 ha areas are governed by hillslope processes related to soil depth, topography, rainfall intensity, and vegetation. Such site factors establish greater variation in the unit area discharge. In contrast, hydrological responses in catchments larger than 100 ha are affected more by routing processes and the structure and extent of floodplains [17]. Finally, disturbances (e.g., landslides, debris flows, and floods) may control the patch distribution of organisms in and around stream systems [19,20]. Montgomery [21] also demonstrated that geomorphic processes set the templates for biological processes of disturbance, river continuum, and patch dynamics using the process–domain concept.

In general, stream water temperature (W_T), as a supplementary tracer, is used to identify and evaluate the water sources contributing to runoff processes at forested catchments [22,23]. W_T fluctuates over time within a given catchment and is also a key driver of drinking water quality and aquatic ecosystem health [24–27]. The natural and anthropogenic mechanisms driving several facets of W_T regimes are also well understood and explain how thermal regimes may vary over time and space [28,29]. Although W_T is generally applied to water quality and aquatic ecosystems [29,30], approaches using both W_T and stream water level (W_L) responses are also effective for identifying event-driven indicators for unexpected rainfall events and flash floods. For instance, Subehi et al. [31] indicated that W_L, which depends on the season and slope gradient, jointly affects the relative proportions of flow paths during rainfall events, thereby influencing changes in specific discharge and water temperature. This is because W_T and W_L are sensitive to climatological and hydrological variables that induce changes in climate or water flow, which may have important implications for W_T and W_L thermal regimes [32,33]. Moreover, we need to consider spatial and temporal variations in hydrologic and geomorphic processes in forested catchments because W_L and W_T are sensitive to vertical distributions between upstream and downstream storm directions [34–36].

Although W_T and W_L can respond to rainfall events and flash floods, the direct application of W_T with W_L as the event-driven indicator has not been fully examined in the forested catchment. Effective application using W_T with W_L can possibly applied for sustainable flood management, which focuses on the role played by ecohydrology in flood risk management. From the ecohydrological perspective, a stream floodplain is an extremely important and capacious ecosystem that, being periodically flooded peaks, may minimize the danger of flooding (e.g., [37–39]). Moreover, when the application is investigated, the hydrological, ecological, and ecotechnological factors can be used to develop sustainable approaches to minimizing flood risk in a given catchment and managing floodplain systems (e.g., [40,41]). According to Rivaes et al. [42], interannual variability is represented by changes in the frequency of floods and variations in annual rainfall, whereas intraannual variability (seasonality) is represented by periods of water surplus interspersed with hydric scarcity. In particular, the frequency and severity of heavy rainfall events in forested catchments have escalated owing to increasing land use and rapid global climate change, with such events frequently resulting in flash flood disasters [43]. Heavy rainfall events often alter environmental conditions, which can influence the composition and structure of biotic communities in terrestrial and aquatic ecosystems [44,45]. In addition, flash floods cause considerable direct and indirect economic losses by damaging socioeconomic systems and infrastructure [46]. In particular, the summer season (mid-June to mid-September), which accounts for 90% of the total rainfall, is concentrated during the East Asian monsoon (late June to mid-September) and typhoons (late July to mid-September) in the Republic of Korea [47–49]. Therefore, assessment of how extreme weather events impact environmental conditions and the consequences for biotic interactions and ecosystem functions and services is critical (e.g., [50]). Such assessed trends have been observed globally, and the damage to the environment is increasing as a result [51,52].

Therefore, there is a significant demand for researchers and governments to construct reliable and accurate flood prediction models and plan and implement sustainable flood risk management measures with an emphasis on prevention and preparedness (e.g., [53]). The objectives of the present were to: (1) examine water level and temperature responses in the time of concentration between rising water level and falling water temperature; (2) identify rising water level and falling water temperature characteristics driven by rainfall events; and (3) determine event-driven indicators using a combination of temperature and water level of stream water in forested catchments.

2. Materials and Methods

2.1. Study Sites

This study was conducted in two catchment categories, including catchment areas less than and or equal to 100 ha ($FC_{\leq 100}$) and catchment areas over 100 ha ($FC_{>100}$), in South Korea (Figure 1). The study area was managed by the National Institute of Forest Science. The distinguishing of two catchment categories was based on structural differences and the continuous versus discontinuous nature of processes [17]. This was because process characteristics differ in the two catchment categories, which needs to be considered when establishing management guidelines for hydrologic, geomorphic, and biological processes in forested catchments [17,54,55].

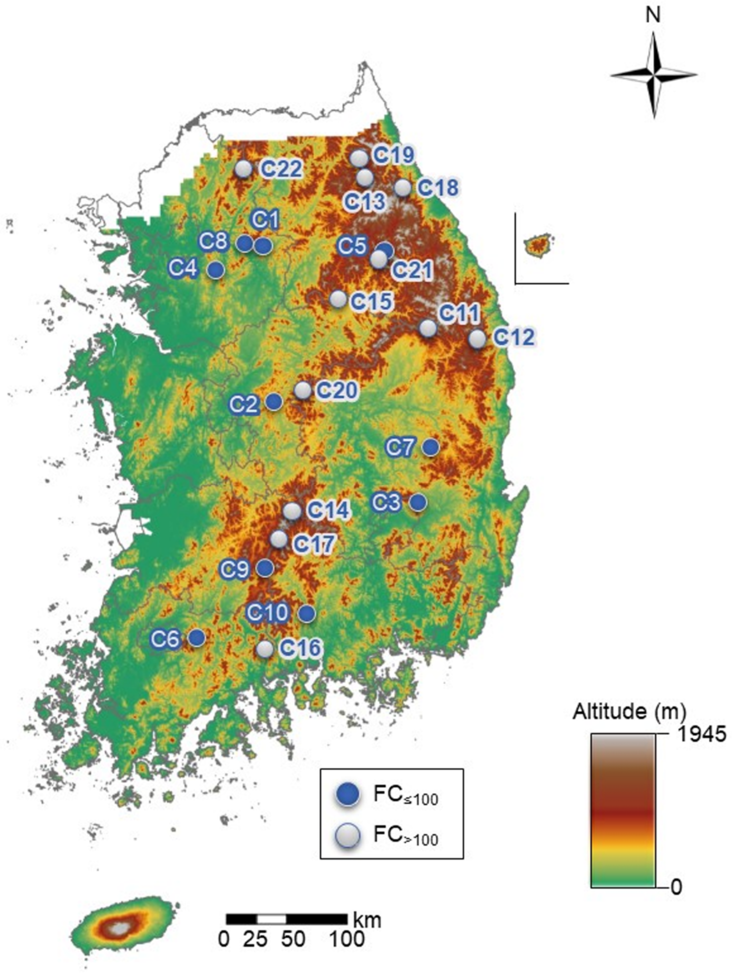

Figure 1. Location of observation sites in ≤100 ha ($FC_{\leq 100}$) and >100 ha ($FC_{>100}$) forested catchments. $FC_{\leq 100}$ and $FC_{>100}$ are included from C1 to C10 and C11 to C22, respectively.

The $FC_{\leq 100}$ areas (C1–C10) were from 13.2 to 59.0 ha, with the altitude ranging from 260 to 1368 m. According to the weather stations of the Korea Meteorological Administration (KMA), the annual precipitation in the regions for 20 years (2003–2022) was 1301.2 ± 370.1 mm (mean ± standard deviation (SD), range: 596.5–2235.2 mm), of which 60%–67% occurred from July to September. The annual temperature was 12.2 ± 1.2 °C (mean ± SD, range: 9.2–14.4 °C). The mean of dominant slope gradients on the $FC_{\leq 100}$

ranged from 20.4 to 34.9°. The underlying geology consists of metamorphic (C1, C4, C6, C8, and C9), sedimentary (C2, C5, and C7), and igneous (C3 and C10) rocks. Most catchments were dominated by deciduous broad-leaved forests, except for C2 and C7, which were covered by mixed forests, and C8, which was covered by coniferous plantations (Table S1).

The $FC_{>100}$ areas (C11–C22) ranged from 101.8 to 281.4 ha, with altitudes ranging from 210 m to 1340 m. According to the weather stations of the KMA, the mean annual precipitation ± SD in the regions for 20 years was 1320.5 ± 345.4 mm (589.2–3000.5 mm), of which 59%–66% occurred from July to September. The mean annual temperature ± SD was 11.2 ± 1.2 °C (9.1–14.4 °C). The mean of dominant slope gradients on the $FC_{\leq 100}$ ranged from 23.4 to 32.8°. The underlying geology consisted of metamorphic (C11, C12, C14–C16, and C18), igneous (C13, C17, C19, C20, and C22), and sedimentary (C21) rocks. Most catchments were dominated by mixed forests, except for C11, C14, and C16, which were covered by broadleaved forests (Table S1).

2.2. Field Measurement and Data Analysis

To investigate stream water temperature and level, a water level gauge was installed at each site in a 90° or 120° V-shaped or square notch. The data were measured using capacitance water stage data loggers (OTT-Orpheus Mini Water Level Logger, OTT Messtechnik, Kempten, Germany) at 10-min intervals. Precipitation was monitored at 10-min intervals using a HOBO tipping-bucket rain gauge (RG3, Onset Computer Corporation, Bourne, MA, USA) in an open area in the study catchment.

Data for the rising stream water level (L_R) in response to falling stream water temperature (T_F) during the observed rainfall events in the summer season (July–September) from 2020 to 2022 were used to indicate event-driven water levels. Here, the L_R was calculated from the minimum to the maximum water level (e.g., [31,56]). The T_F was calculated from the maximum to minimum water temperature. To examine the effects of the time of concentration between T_F and L_R, two types were tested: $T_F = L_R$ and $T_F > L_R$. $T_F = L_R$ indicates the same time of concentration between decreases in stream water temperature (W_T) and increases in stream water level (W_L), and $T_F > L_R$ indicates the fast time of concentration from the decreases in W_T before increasing W_L. We used 25 and 50 observations for $FC_{\leq 100}$ and $FC_{>100}$ for $T_F = L_R$. We used 113 and 158 observations for $FC_{\leq 100}$ and $FC_{>100}$ for $T_F > L_R$. We then estimated the L_R by T_F using regression equations in two catchment categories according to the two types for time of concentration.

The root mean square error (*RMSE*) and Nash-Sutcliffe Efficiency (*NSE*) were selected to evaluate the performances of the estimated L_R in the present study. This was because the *RMSE* and *NSE* alone are not adequate indicators [57]. They are some of the indicators recommended for estimation of efficiency in hydrology (e.g., [58–60]).

The *RMSE* is a commonly used metric for comparing values estimated using the values actually observed [61,62] and was calculated with the following equation:

$$RMSE = \sqrt{\frac{1}{N}\sum_{i=1}^{N}\left(L_{Ri} - \hat{L_{Ri}}\right)^2} \quad (1)$$

where L_{Ri} is the observed L_R at time i (m), $\hat{L_{Ri}}$ is the estimated L_R at time i (m), and N is the total number of rainfall events observed. The *RMSE* can show the estimated errors, with a relatively small value denoting superior estimation [61].

NSE is a trusted tool for evaluating the reliability of developed models [63]. In addition, *NSE* is a normalized statistic that determines the relative magnitude of the residual variance compared to the measured data variance [64] and is computed using the following equation:

$$NSE = 1 - \frac{\sum_{i=1}^{N}\left(L_{Ri} - \hat{L_{Ri}}\right)^2}{\sum_{i=1}^{N}\left(L_{Ri} - \overline{L_{Ri}}\right)^2} \quad (2)$$

$\overline{L_{Ri}}$ is the mean of observed L_R (m). *NSE* ranges from $-\infty$ to 1. As usual, investigators seek an *NSE* value close to 1. A negative *NSE* indicates unacceptable estimated performance [65].

The *RMSE* and *NSE* values were considered accurate when using the estimated L_R as a flood estimation model. Subsequently, the residual was calculated by subtracting the observed L_R from the estimated L_R during a given event in $FC_{\leq 100}$ and $FC_{>100}$ according to the two types of time of concentration. All statistical analyses were performed using R version 4.1.2 (R Foundation for Statistical Computing, Vienna, Austria) and IBM SPSS Statistics 19 (IBM Corp., Armonk, NY, USA).

3. Results and Discussion

3.1. Distribution of Precipitation, Temperature, and Level Responses in Stream Water

The 346 rainfall events were observed over the entire monitoring period, with 75 occurring in the same time of concentration between decreases in stream water temperature (W_T) and increases in stream water level (W_L) ($T_F = L_R$) (Figure 2a) and 271 occurring in the fast time of concentration from the decreases in W_T before increasing W_L ($T_F > L_R$) (Figure 2b). Here, the occurrence of the $T_F > L_R$ was similar in both catchment categories (Figure 2b), whereas the $T_F = L_R$ occurred more in the ≤100 ha ($FC_{\leq 100}$) and >100 ha ($FC_{>100}$) forested catchments (Figure 2a). The falling stream water temperature (T_F) ranged from −3.1 to −0.1 °C, and the rising stream water level (L_R) ranged from 0.001 to 0.9 m. This showed that the W_T decreased by 3.0 °C when W_L increased by up to 0.9 m during rainfall events. Similarly, Irons et al. [66] showed W_T decreases of −1 °C at a 0.10 m W_L for an Alaskan river following precipitation, which was explained by enhanced groundwater upwelling. Hannah et al. [67] indicated a depressed W_T to 0.40 m W_L associated with winter storm flow for a mountain stream. According to Moore [68], W_L is affected by the initial stream source (e.g., groundwater seeps or glaciers), as well as the subsequent effects of energy and water exchanges across the stream water surface.

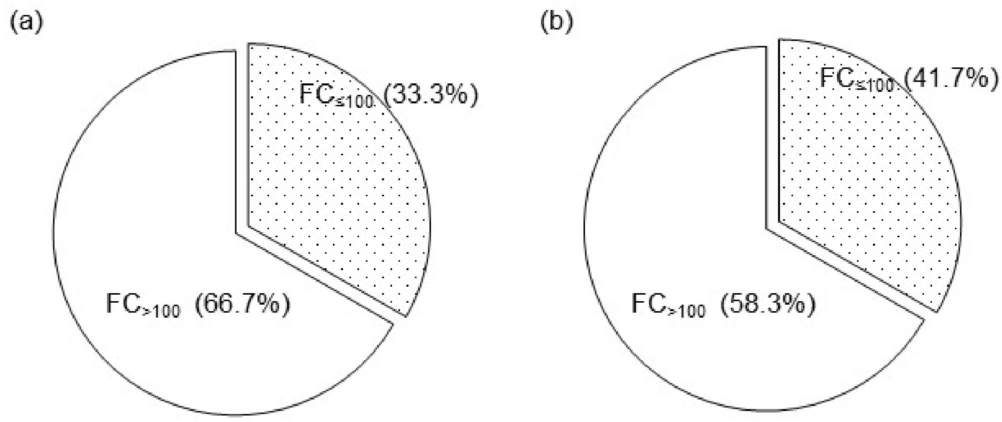

Figure 2. Percentage of different size catchment distributions (i.e., ≤100 ha ($FC_{\leq 100}$) and >100 ha ($FC_{>100}$)) forested catchments in the two types of time of concentration, (**a**) $T_F = L_R$ and (**b**) $T_F > L_R$. $FC_{\leq 100}$ and $FC_{>100}$ are included from C1 to C10 and C11 to C22, respectively.

In the two types of time of concentration, the total precipitation (P_T), W_L, and W_T were compared and analyzed based on the two catchment categories (Table 1 and Figure 3). Figure 3a shows that the T_F of $T_F = L_R$ was −0.4 ± 0.5 °C (mean ± SD) in the $FC_{\leq 100}$ and −0.6 ± 0.6 °C in the $FC_{>100}$. The L_R was 0.1 ± 0.2 m in the $FC_{\leq 100}$ and 0.2 ± 0.2 m in the $FC_{>100}$ with spatial differences between the two catchment categories (Mann–Whitney U test, $p < 0.05$). The mean time of concentration (T_A) was 2.4 and 5.8 h in $FC_{\leq 100}$ and $FC_{>100}$, respectively, with P_T of 14.0 and 33.7 mm. Figure 3b shows that the T_F of the $T_F > L_R$ was −0.3 ± 0.5 °C in the $FC_{\leq 100}$ and −0.4 ± 0.5 °C in the $FC_{>100}$. The L_R was 0.1 ± 0.1 m in the two catchment categories. The time of concentration (T_A) in the T_F was 3.5 and 5.2 h in both $FC_{\leq 100}$ and $FC_{>100}$, respectively, with a P_T of 19.1 and 19.2 mm, respectively. In addition, the mean T_A in the L_R of the $T_F > L_R$ was 5.0 and 6.5 h in the $FC_{\leq 100}$ and $FC_{>100}$, respectively, with a P_T of 25.1 and 23.2 mm, respectively. The spatial differences between the two catchment categories in T_A were significant (Mann–Whitney U test, $p < 0.05$). This could be associated with the steeper slope during repetitive heavy rain and drought processes, which originated from potential direct and/or indirect runoff [68,69]. Because of a small catchment (≤100 ha), which contains ephemeral or temporal channels emerging from zero-order basins [17,70,71], the ephemeral streams flow only as a result of surface runoff generated using precipitation of high intensity and short duration [72]. According to Camarasa-Belmonte and Segura-Beltra [73], the ephemeral runoff, which depends almost exclusively on rainfall, is clearly related to the drainage basin characteristics.

Table 1. Summary of precipitation, temperature, and level in stream water.

		$T_F = L_R$		$T_F > L_R$	
		$FC_{\leq 100}$	$FC_{>100}$	$FC_{\leq 100}$	$FC_{>100}$
T_A (h)	T_F	2.4 ± 2.8 (0.2–12.7)	5.8 ± 4.8 (0.2–20.2)	3.5 ± 3.8 (0.2–16.2)	5.2 ± 5.3 (0.2–23.3)
	L_R			5.0 ± 4.5 (0.3–19.7)	6.5 ± 5.6 (0.3–24.3)
P_T (mm)	T_F	14.0 ± 19.4 (0.5–83.5)	33.7 ± 29.6 (0.5–110.5)	19.1 ± 27.8 (0.4–213.5)	19.2 ± 23.7 (0.5–146.5)
	L_R			25.1 ± 33.3 (1.0–241.0)	23.2 ± 25.7 (0.5–154.5)
W_T (°C)	T_{max}	17.5 ± 1.9 (14.6–21.7)	16.6 ± 2.3 (11.2–21.7)	16.8 ± 2.3 (8.8–22.4)	17.4 ± 2.5 (10.0–22.5)
	T_{min}	17.1 ± 1.7 (14.3–21.5)	16.0 ± 2.2 (10.3–21.0)	16.4 ± 2.2 (8.7–22.3)	17.0 ± 2.5 (9.9–21.9)
	T_F	−0.4 ± 0.5 (−1.9–−0.1)	−0.6 ± 0.6 (−2.4–−0.1)	−0.3 ± 0.5 (−2.3–−0.1)	−0.4 ± 0.5 (−3.1–−0.1)
W_L (m)	L_{min}	0.1 ± 0.1 (0.03–0.4)	0.1 ± 0.1 (0.01–0.5)	0.2 ± 0.2 (0.01–1.2)	0.1 ± 0.1 (0.01–0.6)
	L_{max}	0.2 ± 0.2 (0.03–0.9)	0.3 ± 0.2 (0.03–0.8)	0.3 ± 0.3 (0.01–1.3)	0.3 ± 0.2 (0.01–1.1)
	L_R	0.1 ± 0.2 (0.001–0.7)	0.2 ± 0.2 (0.001–0.7)	0.1 ± 0.1 (0.002–0.9)	0.1 ± 0.1 (0.001–0.7)

Note: $T_F = L_R$: same time of concentration between decreases in stream water temperature (W_T) and increases in stream water level (W_L). $T_F > L_R$: fast time of concentration from the decrease in W_T before increasing W_L. ≤100 ha ($FC_{\leq 100}$) and >100 ha ($FC_{>100}$) forested catchments, T_A: time of concentration, P_T: total precipitation, T_{max}: maximum W_T, T_{min}: minimum W_T, T_F: falling stream water temperature, L_{min}: minimum W_L, L_{max}: maximum W_L, L_R: risings stream water level, ±: SD, bracket: range from minimum to maximum values.

In the two types of time of concentration, the changes in T_F in the $FC_{>100}$ tended to be greater than that in the $FC_{\leq 100}$. Here, the L_R of the $T_F = L_R$ was more altered in the $FC_{>100}$ than in the $FC_{\leq 100}$ (Table 1). It is difficult to perform the first high-temporal-resolution hydrometeorological assessment of the water column and stream thermal variability associated with storm events of different magnitudes, durations, and intensities, not just within a forested basin but also for any catchment-scale effects [56]. Moreover, higher P_T and longer T_A occurred in the $FC_{>100}$ than in the $FC_{\leq 100}$ in the $T_F = L_R$ (Figure 3a). This could be associated with the functional relationships between geomorphic processes in space and time, which are recognized as controls for the continuity of material transport in stream ecosystems [17]. Such dynamics can have potential impacts on the overall aquatic environment as ecological consequences [74,75]. Researchers [76,77] have demonstrated temporal and spatial linkages between hydrologic and geomorphic processes with respect to rainfall–landslide thresholds and channel network development.

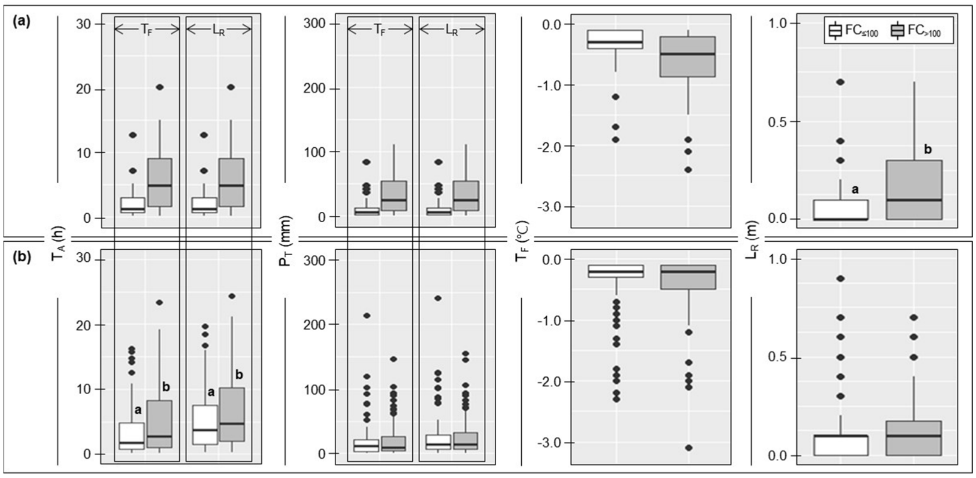

Figure 3. Distribution of time of concentration (T_A) (time of concentration of falling water temperature (T_F), and rising water level (L_R)), total precipitation (P_T) (P_T of T_F and L_R) between ≤100 ha ($FC_{\leq 100}$) and >100 ha ($FC_{>100}$) forested catchments in the two types of time of concentration, (**a**) $T_F = L_R$ and (**b**) $T_F > L_R$. Mann–Whitney U test results are indicated in separate bold letters (**a**,**b**) above the bar graph ($p < 0.05$).

3.2. Factor Affecting Falling Temperature and Rising Levels in Stream Water

Principal component analysis (PCA) was used to analyze the influence parameters considering T_F and L_R responses monitored in the two catchment categories (i.e., ≤100 ha ($FC_{\leq 100}$) and >100 ha ($FC_{>100}$) forested catchments) during the two types of time of concentration (i.e., same time of concentration between decreases in stream water temperature (W_T) and increases in stream water level (W_L) ($T_F = L_R$) and fast time of concentration from the decreases in W_T before increasing W_L ($T_F > L_R$)) using the entire dataset (Table 2 and Figure 4). For the two concentrations, the variance rate was over 90% for Factors 1–3. Table 2 shows the values and proportions of the explained variance and cumulative variance explained by PCA. The PCA identified key parameters of T_F and L_R responses and revealed that major latent factors are influenced by catchment-scale effects. During the two types of time of concentration. In addition, the relative temporal fluctuation of peak flows in small catchments (≤100 ha) was greater than in large catchments ($FC_{>100}$) because storm flow responds rapidly to intense rainfall in small catchments because of their relatively small storage capacity and shorter flow paths [13,17,78].

Table 2. Principal component loadings of six parameters associated with falling temperature and rising level in stream water with total precipitation.

	$T_F = L_R$				$T_F > L_R$			
	Parameter	Factor 1	Factor 2	Factor 3	Parameter	Factor 1	Factor 2	Factor 3
$FC_{\leq 100}$ (C1–C10)	T_A	0.802	0.312	0.439	T_{TF}	0.264	0.870	0.337
					T_{LR}	0.276	0.931	0.091
	P_T	0.939	0.232	0.173	P_{TF}	0.827	0.324	0.380
					P_{LR}	0.911	0.308	0.225
	T_F	−0.305	−0.876	−0.373	T_F	−0.317	−0.242	−0.910
	L_R	0.335	0.498	0.792	L_R	0.930	0.195	0.166
$FC_{>100}$ (C11–C22)	T_A	0.302	0.333	0.890	T_{TF}	0.904	0.268	0.298
					T_{LR}	0.914	0.274	0.253
	P_T	0.907	0.215	0.294	P_{TF}	0.406	0.619	0.595
					P_{LR}	0.356	0.732	0.502
	T_F	−0.249	−0.876	−0.357	T_F	−0.320	−0.327	−0.859
	L_R	0.679	0.623	0.211	L_R	0.233	0.907	0.226

Note: T_F: falling stream water temperature; L_R: rising stream water level; $T_F = L_R$: same time of concentration between decreases in stream water temperature (W_T) and increases in stream water level (W_L). $T_F > L_R$: fast time of concentration from the decrease in W_T before increasing W_L. T_A: time of concentration. T_{LR}: time of concentration of L_R, T_{TF}: time of concentration of T_F, P_T: total precipitation; P_{LR}: total precipitation of L_R, P_{TF}: total precipitation of T_F.

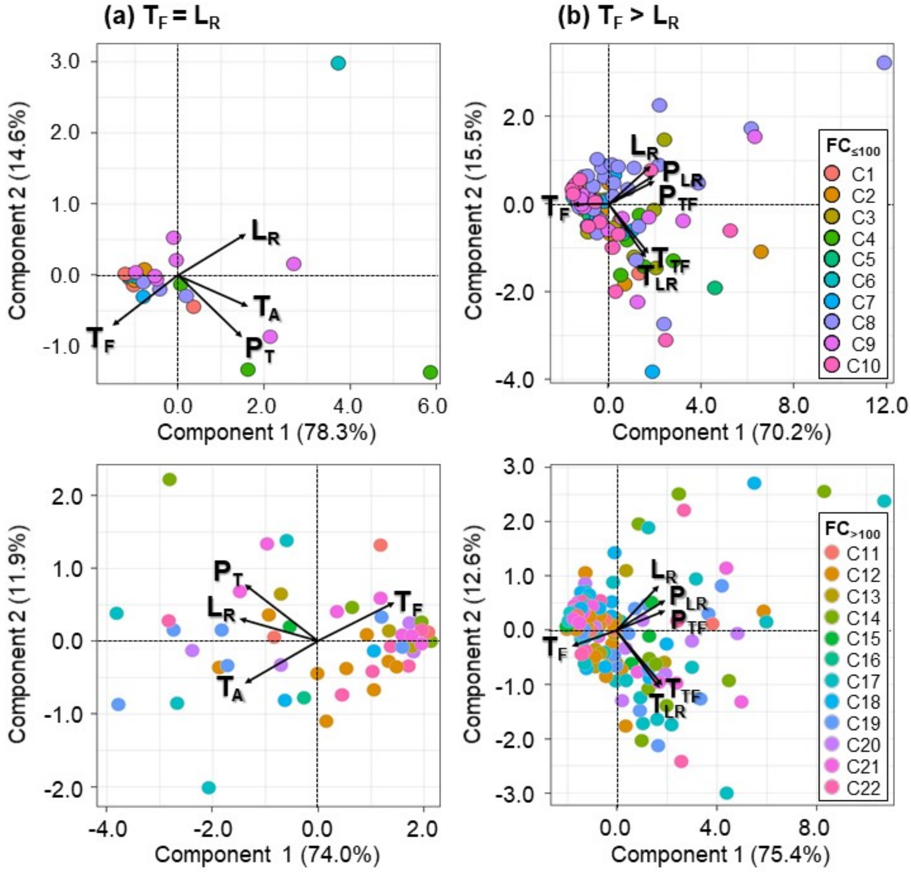

Figure 4. Principal component analysis for six parameters associated with falling stream water temperature (T_F) and rising stream water level (L_R) between ≤100 ha ($FC_{\leq 100}$) and >100 ha ($FC_{>100}$) forested catchments during the two types for the time of concentration, (**a**) $T_F = L_R$ and (**b**) $T_F > L_R$. T_A: time of concentration. T_{LR}: time of concentration of L_R, T_{TF}: time of concentration of T_F, P_T: total precipitation; P_{LR}: total precipitation of L_R, P_{TF}: total precipitation of T_F.

In $T_F = L_R$, the total precipitation (P_T), including time of concentration (T_A) and rising stream water level (L_R), showed high factor loadings for Factor 1, both in $FC_{\leq 100}$ and $FC_{>100}$. This is because flow responses to storms appear to be driven by rapidly routed precipitation (i.e., direct precipitation/channel interception, rapid surface flow over impermeable bedrock/thin alpine soils, and subsurface flow through highly weathered screens) [56]. However, Factor 2 showed that falling stream water temperature (T_F) and L_R had high negative factor loadings in both catchment categories (Figure 4a). It is most likely that the stream temperature response to P_T results from advected energy inputs, primarily from the surface and near-subsurface hillslope pathways [56]. In addition, climatic drivers, stream morphology, groundwater influence, and riparian canopy conditions reportedly affect stream thermal regimes [28,29,79]. In $T_F > L_R$, high factor loadings for Factors 1–3 differed according to the catchment category; however, T_F was Factor 3 in both catchment categories (Figure 4b). It seemed that factors affecting the T_F and L_R responses were difficult to identify exactly in the $T_F > L_R$.

3.3. *Relationship between Falling Temperature and Rising Level in Stream Water*

To evaluate the correlations among the monitoring data between ≤100 ha ($FC_{\leq 100}$) and >100 ha ($FC_{>100}$) forested catchments in the same time of concentration between decreases in stream water temperature (W_T) and increases in stream water level (W_L) ($T_F = L_R$) and the fast time of concentration from the decreases in W_T before increasing W_L ($T_F > L_R$), correlation analyses were performed for a time of concentration (T_A), total precipitation

(P_T), falling stream water temperature (T_F), and rising stream water level (L_R) characteristics (Table 3).

Table 3. Correlation matrix for total precipitation, falling temperature, and rising level in stream water.

T_F = L_R													
		T_A	P_T	T_F					T_A	P_T	T_F		
$FC_{\leq 100}$ (*n* = 25)	P_T	**0.85**					$FC_{>100}$ (*n* = 50)	P_T	**0.59**				
	T_F	**−0.69**	**−0.55**					T_F	**−0.67**	**−0.56**			
	L_R	**0.74**	**0.59**	**−0.83**				L_R	**0.63**	**0.74**	**−0.72**		
T_F > L_R													
		T_{TF}	T_{LR}	P_{TF}	P_{LR}	T_F			T_{TF}	T_{LR}	P_{TF}	P_{LR}	T_F
$FC_{\leq 100}$ (*n* = 113)	T_{LR}	**0.86**					$FC_{>100}$ (*n* = 158)	T_{LR}	**0.95**				
	P_{TF}	**0.65**	**0.54**					P_{TF}	**0.72**	**0.66**			
	P_{LR}	**0.57**	**0.56**	**0.95**				P_{LR}	**0.65**	**0.66**	**0.93**		
	T_F	**−0.58**	**−0.42**	**−0.66**	**−0.57**			T_F	**−0.63**	**−0.61**	**−0.78**	**−0.74**	
	L_R	**0.47**	**0.46**	**0.84**	**0.91**	**−0.51**		L_R	**0.53**	**0.53**	**0.73**	**0.79**	**−0.63**

Note: T_F = L_R: same time of concentration between decreases in stream water temperature (W_T) and increases in stream water level (W_L). T_F > L_R: fast time of concentration from the decrease in W_T before increasing W_L. ≤100 ha ($FC_{\leq 100}$) and >100 ha ($FC_{>100}$) forested catchments, T_A: time of concentration, P_T: total precipitation, T_{max}: maximum W_T, T_{min}: minimum W_T, T_F: falling stream water temperature, L_{min}: minimum W_L, L_{max}: maximum W_L, L_R: rising stream water level, ±: SD, bracket: range from minimum to maximum values. Significant correlations are shown in bold type.

To assess the correlation between the characteristics in the two catchment categories, the significance level was set at 0.01 or less, which implied a high correlation. The results are summarized in Table 3. Here, the L_R of T_F = L_R was positively correlated with T_A and P_T in both catchments (correlation coefficient: 0.59–0.74, $p < 0.01$). The L_R of the T_F > L_R also showed a significant correlation with T_A and P_T parameters (correlation coefficient: 0.46–0.91, $p < 0.01$). However, the T_F of the two types for the time of concentration was negatively correlated with T_A, P_T, and L_R, with correlation coefficients ranging from −0.78 to −0.42 in both catchment categories ($p < 0.01$) (Table 3). Previous studies have indicated that P_T has the greatest influence on stream water with seasonal changes [68,80,81]. The researchers [23,56] also discussed that P_T may cause changes in W_L owing to direct inputs (i.e., channel interception) and by inducing W_L from various hydrological stores and pathways. Lee et al. [82] showed that annual variations in streamflow timing and volume depend on the seasonal cycles of P_T in the upper part of the basin. Thus, P_T can affect changes in the temperature and level of stream water as a function of climate variability within a catchment (e.g., [83,84]), even if T_F and L_R have different correlation patterns.

In the two types of time of concentration, T_F decreased with increasing L_R in both catchment categories. The L_R and T_F patterns were similar in both catchment categories in the T_F = L_R (Figure 5a). In the T_F > L_R, the L_R with T_F patterns of the $FC_{>100}$ was larger than that of the $FC_{\leq 100}$ (Figure 5b). This was due to spatial and temporal differences in thermal response to storm events, which were controlled by P_T and W_L [23,31,56]. Brown and Hannah [56] discussed that the catchment characteristics influencing event-driven thermal variability can be speculated upon at present because temperature data are not routinely collected in studies of runoff generation processes. In addition, according to Oware and Peterson [85], storm events strongly influence W_T in the direction of the pre-storm thermal gradient between the stream and substrate temperatures. Furthermore, storm flow responds rapidly to intense rainfall in the $FC_{\leq 100}$ because of their relatively low storage capacity and shorter flow paths [17]. Storm flow generation in the $FC_{\leq 100}$ is also affected by the responses of hillslopes and zero-order basins to changing antecedent moisture conditions [86,87]. In other words, the relationship between T_F and L_R can be combined with the response to the stream surface energy balance and catchment-scale effects. The T_F is, therefore, less sensitive to uncertainties in precipitation, whereas these uncertainties potentially have a large impact on the simulated L_R (e.g., [88–90]). Our methodological approach using relationships between temperature and water level could facilitate the formulation of sustainable flood management strategies with variations in commonly used spatial and temporal scales (e.g., [56,91]).

Table 4. Summary of regression analyses to estimate rising stream water levels.

		Equation	R^2	*n*	*F*	*p*
$T_F = L_R$	$FC_{\leq 100}$	$L_R = -0.278(T_F) - 0.021$	0.69	25	51.60	<0.001
	$FC_{>100}$	$L_R = -0.259(T_F) + 0.024$	0.52	50	52.24	<0.001
$T_F > L_R$	$FC_{\leq 100}$	$L_R = -0.162(T_F) + 0.051$	0.26	113	38.98	<0.001
	$FC_{>100}$	$L_R = -0.199(T_F) + 0.035$	0.39	158	100.09	<0.001

Note: T_F: falling stream water temperature; L_R: rising stream water level; $T_F = L_R$: same time of concentration between decreases in stream water temperature (W_T) and increases in stream water level (W_L). $T_F > L_R$: fast time of concentration from the decrease in W_T before increasing W_L. ≤100 ha ($FC_{\leq 100}$) and >100 ha ($FC_{>100}$) forested catchments.

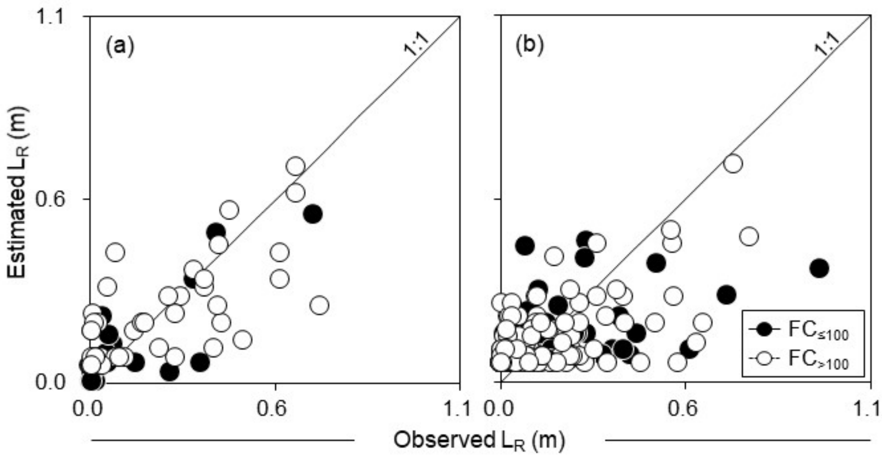

Figure 5. Relationship between falling stream water temperature (T_F) and rising stream water level (L_R) between ≤100 ha ($FC_{\leq 100}$) and >100 ha ($FC_{>100}$) forested catchments during the two types for the time of concentration, (**a**) $T_F = L_R$ and (**b**) $T_F > L_R$. Thick and broken lines were estimated using regression analysis (see Table 4) for two catchment categories.

3.4. Approaches to Estimating Rising Levels Using Falling Temperature in Stream Water

Table 4 shows the regression analysis results for the two catchment categories at the same time of concentration between decreases in stream water temperature (W_T) and increases in stream water level (W_L) ($T_F = L_R$). Significant results were obtained, with coefficients of determination (R^2) ranging from 0.52 to 0.69 at a 99% significance level. On the other hand, the two equations in the fast time of concentration from the decreases in W_T before increasing W_L ($T_F > L_R$) did not have a relatively fit to estimate rising stream water level (L_R) using falling stream water temperature (T_F).

The estimated L_R (mean ± SD) in the $T_F = L_R$ was 0.1 ± 0.1 m (range: 0.01–0.5 m) and 0.2 ± 0.1 m (0.05–0.6 m) in the $FC_{\leq 100}$ and $FC_{>100}$, respectively (Figure 6a). In the $T_F > L_R$, the estimated L_R (mean ± SD) was similar to 0.1 ± 0.1 m (0.1–0.4 m and 0.1–0.7 m in the $FC_{\leq 100}$ and $FC_{>100}$) in both catchment categories (Figure 6b). As illustrated in Figure 6, the relationship between the observed and estimated L_R was suitable for determining the event-driven indicator using a combination of temperature and level of stream water, particularly when the L_R was estimated using the T_F in the two catchment categories in $T_F = L_R$ (Figure 6a). The differences may have been caused by the time of concentration between the T_F and L_R with catchment scale effects. Stream and event flow generation processes modify the biological community structure and life cycle of aquatic fauna from upstream to downstream systems [92–95]. Therefore, the estimated L_R of the two catchment categories was greater when $T_F = L_R$ than when $T_F > L_R$. In particular, during the $T_F = L_R$, the estimated L_R in the $FC_{\leq 100}$ was greater than that in the $FC_{>100}$ because water inputs strongly affect hillslope and channel conditions because of the close coupling of hydrologic and geomorphic processes within confined and steep valleys of $FC_{\leq 100}$ [87]. Water temperature in stream channels is closely related to the soil pore structure and bedrock fractures in hillslopes and zero-order basins [17]. In the $FC_{\leq 100}$, subsurface discharge from hillslopes contributes base flow and storm flow to stream channels, initiates certain erosion processes, and is important for the development of catchment topography [77].

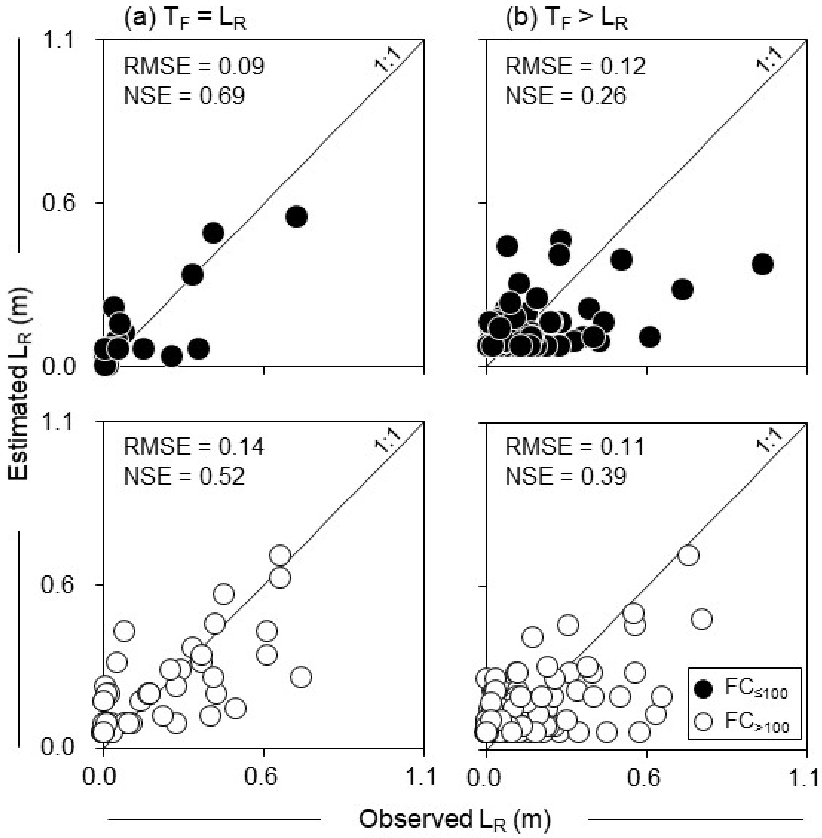

Figure 6. Relationship between the observed and estimated rising stream water level between ≤100 ha ($FC_{\leq 100}$) and >100 ha ($FC_{>100}$) forested catchments during the two types of time of concentration, (**a**) $T_F = L_R$ and (**b**) $T_F > L_R$.

The residual between the observed and estimated L_R during the $T_F = L_R$ ranged from −0.2 to 0.3 m and −0.3 to 0.5 m in the $FC_{\leq 100}$ and $FC_{>100}$, respectively (Figure 7a). In the $T_F > L_R$, the residual is within a similar range, at −0.3–0.6 m and −0.2–0.5 m in the $FC_{\leq 100}$ and $FC_{>100}$, respectively (Figure 7b). When the $T_F = L_R$, the NSE values were 0.69 and 0.52 with 0.09 and 0.14 RMSE values in the two catchment categories (Figure 6a), the estimated accuracy on the $FC_{\leq 100}$ was higher than that of the $FC_{>100}$ (Figure 7a). In contrast, the NSE values with RMSE in the $T_F > L_R$ were 0.26 with 0.12 and 0.39 with 0.11 in the $FC_{\leq 100}$ and $FC_{>100}$ (Figure 6b), respectively, i.e., the estimated accuracy was low (Figure 7b).

Therefore, the above results indicate that the estimated L_R was appropriate in small catchments ($FC_{\leq 100}$) during the $T_F = L_R$. Subehi et al. [31] indicated that change in W_T is influenced more by changes in specific W_L. Our estimated rising stream water level was appropriate in small catchments (≤100 ha) and could be included in the expansion of hydrologically active areas (e.g., riparian zones, zero-order basins, and bogs) during periods of increasing wetness, which increases the probability of mass movements and alters flow paths between terrestrial and aquatic environments [17,31,96,97]. Therefore, hydrologists studying rainfall-runoff processes in catchment scale effects, particularly small catchments (≤100 ha) (e.g., [17,87,98]) could greatly contribute to the understanding of the processes incorporating W_T measurements alongside W_L and confirm the application of W_T with W_L as event-driven indicators in the forested catchments.

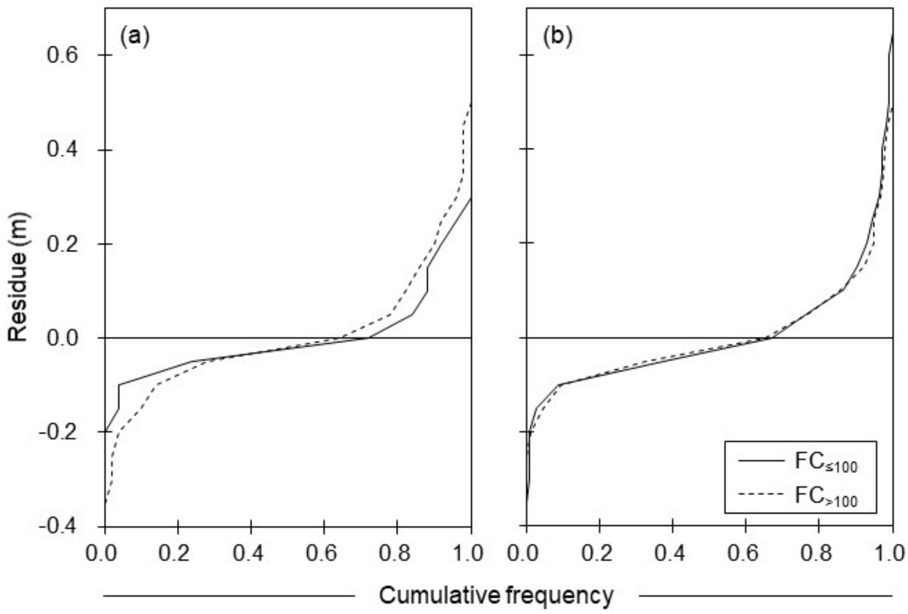

Figure 7. Cumulative frequency distributions for differences between observed and estimated rising water levels between ≤100 ha ($FC_{\leq 100}$) and >100 ha ($FC_{>100}$) forested catchments in the two types of time of concentration, (**a**) $T_F = L_R$ and (**b**) $T_F > L_R$.

4. Summary and Conclusions

We investigated event flow characteristics based on the level and temperature of stream water during 346 rainfall events across the summer season (July–September) from 2020 to 2022 in 22 forested catchments (area: 13.2–281.4 ha). To indicate event-driven water levels, we used event data for rising stream water levels (L_R) that responded to falling stream water temperature (T_F) between ≤100 ha ($FC_{\leq 100}$) and >100 ha ($FC_{>100}$) forested catchments in the two types of time of concentration (i.e., $T_F = L_R$ and $T_F > L_R$). Our main findings are as follows: (1) stream water temperature decreased by 3.0 °C, when stream water level increased by up to 0.9 m; (2) the falling stream water temperature in the two types of time of concentration was negatively correlated with total precipitation and rising stream water level (correlation coefficient: −0.78–0.42, $p < 0.01$) due to water column and stream thermal variability associated with storm events; (3) the T_F decreased with increasing L_R in both catchment categories at both types of time of concentration; (4) in addition, the rising stream water level pattern of the $FC_{>100}$ was greater, due to changes in falling stream water temperature, than that of the $FC_{\leq 100}$ in the $T_F > L_R$, due to combined effects of stream surface energy balance and catchment scale effects in response to the start of rainfall; and (5) based on relative high regression and cumulative frequency distribution, the estimated rising stream water level was appropriate for a small catchment (≤100 ha) during the same time of concentration between decreases in stream water temperature and increase in stream water level during rainfall events. This could be associated with the expansion of hydrologically active areas (e.g., riparian zones, zero-order basins, and bogs) during concentrated rainfall periods, which alter the flow paths between terrestrial and aquatic environments in forested catchments. Our results indicate that the unique aspects of our study design allowed us to draw inferences about event flow characteristics based on the contribution of temperature and stream water level in small catchments (≤100 ha) during the time of concentration sequences. Furthermore, our results could facilitate the integration of the falling curve of stream water temperature in response to rising stream water levels, which need to consider the catchment-scale effects, particularly in the small catchments (≤100 ha) for aquatic ecosystem and event-driven indicators of the potential environmental and ecological consequences.

Supplementary Materials: The following supporting information can be downloaded at: https://www.mdpi.com/article/10.3390/f14102085/s1, Table S1: Summary of observed sites in forested catchments.

Author Contributions: Conceptualization, S.N. and H.T.C.; methodology, S.N. and H.L.; software, S.N., H.L., and H.T.C.; validation, S.N.; formal analysis, S.N. and H.L.; investigation, S.N., H.L., B.C., and H.T.C.; resources, S.N., H.L., and H.T.C.; data curation, S.N., H.L., and H.T.C.; writing—original draft preparation, S.N. and H.T.C.; writing—review and editing, S.N., B.C., Q.L. and H.M.; visualization, S.N., H.L., and B.C.; supervision, S.N. and H.T.C.; project administration, S.N., H.L., B.C., and H.T.C.; funding acquisition, H.T.C. All authors have read and agreed to the published version of the manuscript.

Funding: This study was carried out with the support of the "R&D Program for Forest Science Technology (Project No. 2021343B10-2323-CD01)" provided by the Korea Forest Service (Korea Forestry Promotion Institute).

Data Availability Statement: Not applicable.

Conflicts of Interest: The authors declare they have no conflict of interest.

References

1. Intergovernmental Panel on Climate Change (IPCC). *Climate Change 2007: The Physical Science Basis-Summary for Policy Makers. Contribution of Working Group I to the Fourth Assessment Report of the Intergovernmental Panel on Climate Change*; IPCC WGI 4th Assessment Report; IPCC: Cambridge, UK, 2007.
2. McMichael, A.J.; Lindgren, E. Climate change: Present and future risks to health, and necessary responses. *J. Intern. Med.* **2011**, *270*, 401–413. [CrossRef] [PubMed]
3. Intergovernmental Panel on Climate Change (IPCC). *Climate Change 2014: Mitigation of Climate Change*; Cambridge University Press: Cambridge, UK; New York, NY, USA, 2014; Volume 3.
4. Kim, Y.H.; Kim, E.S.; Choi, M.J.; Shim, K.M.; Ahn, J.B. Evaluation of long-term seasonal predictability of heatwave over South Korea using PNU CGCM-WRF Chain. *Atmosphere* **2019**, *29*, 671–687. (In Korean)
5. Ahn, J.J. Lessons learned from major environmental health disasters in South Korea and the role of environmental health experts. *J. Environ. Health Sci.* **2022**, *48*, 9–18. (In Korean) [CrossRef]
6. Wu, X.; Lu, Y.; Zhou, S.; Chen, L.; Xu, B. Impact of climate change on human infectious diseases: Empirical evidence and human adaptation. *Environ. Int.* **2016**, *86*, 14–23. [CrossRef]
7. Frederick, K.D.; Major, D.C. Climate change and water resources. *Clim. Change* **1997**, *37*, 7–23. [CrossRef]
8. Arnell, N.W. Climate change and global water resources. *Glob. Environ. Change* **1999**, *9*, S31–S49. [CrossRef]
9. Dey, D.; Mishra, A. Separating the impacts of climate change and human activities on streamflow: A review of methodologies and critical assumptions. *J. Hydrol.* **2017**, *548*, 278–290. [CrossRef]
10. Kim, I.J.; Han, D.H. *A Small Stream Management Plan to Protect the Aquatic Ecosystem*; RE-09; Korea Environment Institute (KEI): Sejong, Republic of Korea, 2008; p. 149. (In Korean)
11. Korea Forest Service (KFS). *Statistical Yearbook of Forestry 2019*; Korea Forest Service: Daejeon, Republic of Korea, 2019; p. 444. (In Korean)
12. Jun, J.H.; Kim, K.H.; Yoo, J.Y.; Choi, H.T.; Jeong, Y.H. Variation of suspended solid concentration, electrical conductivity and pH of stream water in the regrowth and rehabilitation forested catchments, South Korea. *J. Korean Soc. For. Sci.* **2007**, *96*, 21–28. (In Korean)
13. Robinson, C.T.; Tonolla, D.; Imhof, B.; Vukelic, R.; Uehling, U. Flow intermittency, physico-chemistry and function of headwater streams in an Alpine glacial catchment. *Aquat. Sci.* **2016**, *78*, 327–341. [CrossRef]
14. Kim, D.Y. Effect of regional climate change on precipitation in the 21st century. *J. Korean Soc. Environ. Technol.* **2020**, *21*, 205–210. (In Korean) [CrossRef]
15. Gillham, R.W. The capillary fringe and its effect on watertable response. *J. Hydrol.* **1984**, *67*, 307–324. [CrossRef]
16. Woods, R.; Sivapalan, M.; Duncan, M. Investigating the representative elementary area concept: An approach based on field data. *Hydrol. Process.* **1995**, *9*, 291–312. [CrossRef]
17. Gomi, T.; Sidle, R.C.; Richardson, J.S. Understanding processes and downstream linkages of headwater systems. *Bioscience* **2002**, *52*, 905–916. [CrossRef]
18. Wood, E.F.; Sivapalan, M.; Beven, K.; Band, L. Effects of spatial variability and scale with implications to hydrologic modeling. *J. Hydrol.* **1988**, *102*, 29–47. [CrossRef]
19. Townsend, C.R. The patch dynamics concept of stream community ecology. *J. N. Am. Benthol. Soc.* **1989**, *8*, 36–50. [CrossRef]
20. Gregory, S.V.; Swanson, F.J.; McKee, W.A.; Cummins, K.W. An ecosystems perspective of riparian zones. *BioScience* **1991**, *41*, 540–551. [CrossRef]
21. Montgomery, D.R. Process domain and river continuum. *J. Am. Water Resour. Assoc.* **1999**, *35*, 397–410. [CrossRef]

22. Shanley, J.B.; Peters, N.E. Preliminary observations of streamflow generation during storms in a forested Piedmont watershed using temperature as a tracer. *J. Contam. Hydrol.* **1988**, *3*, 349–365. [CrossRef]
23. Kobayashi, D.; Ishii, Y.; Kodama, Y. Stream temperature, specific conductance and runoff process in mountain watersheds. *Hydrol. Process.* **1999**, *13*, 865–876. [CrossRef]
24. Dallas, H.; Day, J.; Musibono, D.; Day, E. Water quality for aquatic ecosystems: Tools for evaluating regional guidelines. *WRC Rep.* **1998**, *626*, 98–240.
25. Arismendi, I.; Johnson, S.L.; Dunham, J.B.; Haggerty, R. Descriptors of natural thermal regimes in streams and their responsiveness to change in the Pacific Northwest of North America. *Freshw. Biol.* **2013**, *58*, 880–894. [CrossRef]
26. Fullerton, A.H.; Torgerse, C.E.; Lawler, J.J.; Faux, R.N.; Steel, E.A.; Beechie, T.J.; Ebersole, J.L.; Leibowitz, S.G. Rethinking the longitudinal stream temperature paradigm: Region-wide comparison of thermal infrared imagery reveals unexpected complexity of river temperatures. *Hydrol. Process.* **2015**, *29*, 4719–4737. [CrossRef]
27. Agudelo-Vera, C.; Avvedimento, S.; Boxall, J.; Creaco, E.; de Kater, H.; Di Nardo, A.; Djukic, A.; Douterelo, I.; Fish, K.; Iglesias Rey, P.L. Drinking water temperature around the global: Understanding, policies, challenges and opportunities. *Water* **2020**, *12*, 1049. [CrossRef]
28. Caissie, D. The thermal regime of rivers: A review. *Freshw. Biol.* **2006**, *51*, 1389–1406. [CrossRef]
29. Webb, B.W.; Hannah, D.W.; Moore, R.D.; Brown, L.E.; Nobilis, F. Recent advances in stream and river temperature research. *Hydrol. Process.* **2008**, *22*, 902–918. [CrossRef]
30. Nam, S.; Jang, S.J.; Chun, K.W.; Lee, J.U.; Kim, S.W. Seasonal water temperature variations in response to air temperature and precipitation in a forested headwater stream and an urban river: A case study from the Bukhan River basin, South Korea. *Forest Sci. Technol.* **2021**, *17*, 46–55. [CrossRef]
31. Subehi, L.; Fukushima, T.; Onda, Y.; Mizugaki, S.; Gomi, T.; Kosugi, K.; Hiramatsu, S.; Kitahara, H.; Kuraji, K.; Terajima, T. Analysis of stream water temperature changes during rainfall events in forested watersheds. *Limnology* **2010**, *11*, 115–124. [CrossRef]
32. Webb, B.W.; Clack, P.D.; Walling, D.E. Water–air temperature relationships in a Devon river system and the role of flow. *Hydrol. Process.* **2003**, *17*, 3069–3084. [CrossRef]
33. Brown, L.E.; Hannah, D.M.; Milner, A.M. Hydroclimatological influences on water column and streambed thermal dynamics in an alpine river system. *J. Hydrol.* **2006**, *325*, 1–20. [CrossRef]
34. Watts, L.G.; Calver, A. Effects of spatially-distributed rainfall on runoff for a conceptual catchment. *Nord. Hydrol.* **1991**, *22*, 1–14. [CrossRef]
35. Poole, G.C.; Berman, C.H. An ecological perspective on the in-stream temperature: Natural heat dynamics and mechanisms of human-caused thermal degradation. *Environ. Manag* **2001**, *14*, 621–628. [CrossRef]
36. Feng, Y.; Brubaker, K.L. Sensitivity of flood-depth frequency to watershed-runoff change and sea-level rise using a one-dimensional hydraulic model. *J. Hydrol. Eng.* **2016**, *21*, 05016015. [CrossRef]
37. Arrow, K.; Bolin, B.; Costanza, R.; Dasgupta, P.; Folke, C.; Holling, C.S.; Jansson, B.-O.; Levin, S.; Ma¨ler, K.-G.; Perrings, C.; et al. Economic growth, carrying capacity, and the environment. *Ecol. Econ.* **1995**, *15*, 91–95. [CrossRef]
38. Kaczorowski, D.; Sekulska-Nalewajko, J.; Kiedrzyńska, E. Three-dimensional model of flooding of the river floodplain—visualization of ecohydrological interactions. In *Perspective Technologies and Methods in MEMS Design, Proceedings of the 2nd International Conference of Young Scientists, MEMSTECH 2006, Lviv, Ukraine, 24–27 May 2006*; IEEE: New York, NY, USA, 2006; pp. 146–148.
39. Kiedrzynska, E.; Kiedrzynski, M.; Zalewski, M. Sustainable floodplain management for flood prevention and water quality improvement. *Nat. Hazards* **2015**, *76*, 955–977. [CrossRef]
40. Zalewski, M.; Janauer, G.S.; Jolankai, G. *Ecohydrology—A New Paradigm for the Sustainable Use of Aquatic Resources*; Technical Document on Hydrology; International Hydrological Program UNESCO: Paris, France, 1997.
41. Zalewski, M. Flood pulses and river ecosystem robustness. In *Frontiers in Flood Research*; Kovacs colloquium; Tchiguirinskaia, I., Thein, K.N.N., Hubert, P., Eds.; IAHS Publication: Port Elizabeth, South Africa; UNESCO: Paris, France, 2006; p. 212.
42. Rivaes, R.; Rodríguez-González, P.M.; Albuquerque, A.; Pinheiro, A.N.; Egger, G.; Ferreira, M.T. Riparian vegetation responses to altered flow regimes driven by climate change in Mediterranean rivers: Riparian vegetation responses to altered flow regimes. *Ecohydrology* **2013**, *6*, 413–424. [CrossRef]
43. Tabari, H. Climate change impact on flood and extreme precipitation increases with water availability. *Sci. Rep.* **2020**, *10*, 13768. [CrossRef] [PubMed]
44. Jentsch, A.; Kreyling, J.; Beierkhunlein, C. A new generation of climate-change experiments: Events, not trends. *Front. Ecol. Environ.* **2007**, *5*, 365–374. [CrossRef]
45. Lawson, C.R.; Vindenes, Y.; Bailey, L.; van de Pol, M. Environmental variation and population responses to global change. *Ecol. Lett.* **2015**, *18*, 724–736. [CrossRef] [PubMed]
46. Sieg, T.; Schinko, T.; Vogel, K.; Mechler, R.; Merz, B.; Kreibich, H. Integrated assessment of short-term direct and indirect economic flood impacts including uncertainty quantification. *PLoS ONE* **2019**, *14*, e0212932. [CrossRef]
47. Chang, H.; Franczyk, J.; Im, E.S.; Kwon, W.T.; Bae, D.H.; Jung, I.W. Vulnerability of Korean water resources to climate change and population growth. *Water Sci. Technol.* **2007**, *56*, 57–62. [CrossRef]

48. Bae, S.K.; Kim, Y.H. Estimation of groundwater recharge rate using the NRCS-CN and the baseflow separation methods. *J. Environ. Sci. Int.* **2006**, *15*, 253–260. (In Korean)
49. Lee, J.Y.; Jeon, W.H.; Park, Y.; Lim, H.G. Status and prospect of groundwater resources in Pyeongchang, Gangwon-do. *J. Geo. Soc. Korea* **2012**, *48*, 435–444. (In Korean)
50. Cardinale, B.J.; Duffy, J.E.; Gonzalez, A.; Hooper, D.U.; Perrings, C.; Venail, P.; Kinzig, A.P. Biodiversity loss and its impact on humanity. *Nature* **2012**, *486*, 59–67. [CrossRef] [PubMed]
51. Teuling, A.J.; De Badts, E.A.; Jansen, F.A.; Fuchs, R.; Buitink, J.; Hoek van Dijke, A.J.; Sterling, S.M. Climate change, reforestation/afforestation, and urbanization impacts on evapotranspiration and streamflow in Europe. *Hydrol. Earth Syst. Sci.* **2019**, *23*, 3631–3652. [CrossRef]
52. Gulahmadov, N.; Liu, T.; Anjum, M.N.; Rizwan, M. Simulation of the potential impacts of projected climate change on streamflow in the Vakhsh River basin in central Asia under CMIP5 RCP scenarios. *Water* **2020**, *12*, 1426. [CrossRef]
53. Danso-Amoako, E.; Scholz, M.; Kalimeris, N.; Yang, Q.; Shao, J. Predicting dam failure risk for sustainable flood retention basins: A generic case study for the wider Greater Manchester area. *Comput. Environ. Urban Syst.* **2012**, *36*, 423–433. [CrossRef]
54. Montgomery, D.R.; Foufoula-Georgiou, E. Channel network source representation using digital elevation models. *Water Resour. Res.* **1993**, *29*, 3925–3934. [CrossRef]
55. Swanson, F.J.; Johnson, S.L.; Gregory, S.V.; Acker, S.A. Flood disturbance in a forested mountain landscape. *BioScience* **1998**, *48*, 681–689. [CrossRef]
56. Brown, L.E.; Hannah, D.M. Alpine stream temperature response to storm events, J. *Hydrometeorol.* **2007**, *8*, 952–967. [CrossRef]
57. Jain, S.; Sudheer, K. Fitting of hydrologic models: A close look at the Nash–Sutcliffe Index. *J. Hydrol. Eng.* **2008**, *13*, 981–986. [CrossRef]
58. Sevat, E.; Dexetter, A. Selection of calibration objective functions in the context of rainfall-runoff modeling in a Sudanese Savannah Area. *Hydrol. Sci. J.* **1991**, *36*, 307–330. [CrossRef]
59. Legates, D.R.; McCabe, G.J. Evaluating the use of 'Goodness-of-Fit' measures in hydrologic and hydroclimatic model validation. *Water Resour. Res.* **1999**, *35*, 233–241. [CrossRef]
60. Singh, J.; Knapp, H.V.; Demissie, M. Hydrologic modeling of the Iroquois River Watershed using HSPF and SWAT. *J. Am. Water Resour. Assoc.* **2005**, *41*, 361–375. [CrossRef]
61. Willmott, C.J.; Matsuura, K. Advantages of the mean absolute error (MAE) over the root mean square error (RMSE) in assessing average model performance. *Clim. Res.* **2005**, *30*, 79–82. [CrossRef]
62. Yndman, R.J. Another look at forecast accuracy metrics for intermittent demand. *Foresight* **2006**, *4*, 43–46.
63. Chen, H.; Xu, C.Y.; Guo, S. Comparison and evaluation of multiple GCMs, statistical downscaling and hydrological models in the study of climate change impacts on runoff. *J. Hydrol.* **2012**, *434–435*, 36–45. [CrossRef]
64. Nash, J.E.; Sutcliffe, J.V. River flow forecasting through conceptual models Part I—A discussion of principles. *J. Hydrol.* **1970**, *10*, 282–290. [CrossRef]
65. Zhong, W.; Dutta, U. Engaging Nash-Sutcliffe efficiency and model efficiency factor indicators in selecting and validating effective light rail system operation and maintenance cost models. *J. Traffic Transport. Eng.* **2015**, *3*, 255–265.
66. Irons, J.G.; Ray, S.R.; Miller, L.K.; Oswood, M.W. Spatial and seasonal patterns of streambed water temperatures in an Alaskan subarctic stream. In Proceedings of the Symposium on Headwaters Hydrology, Merano, Italy, 20–23 April 1998; American Water Resources Association: Bethesda, MD, USA, 1989; pp. 381–390.
67. Hannah, D.M.; Malcolm, I.A.; Soulsby, C.; Youngson, A.F. Heat exchanges and temperatures within a salmon spawning stream in the Cairngorms, Scotland: Seasonal and sub-seasonal dynamics. *River Res. Appl.* **2004**, *20*, 635–652. [CrossRef]
68. Moore, R.D. Stream temperature patterns in British Columbia, Canada, based on routine spot measurements. *Can. Water Resour. J.* **2006**, *31*, 41–56. [CrossRef]
69. Park, J.C.; Lee, H.H. Variations of stream water quality caused by discharge change. *J. Korean For. Soc.* **2000**, *89*, 342–355. (In Korean)
70. Anderson, N.H. Phenology of Trichoptera in summer-dry headwater streams in western Oregon, U.S.A. In Proceedings of the 8th International Symposium on Trichoptera, Lake Itasca, MN, USA, 9–15 August 1995; Holzenthal, R.W., Flint, O.S., Eds.; Ohio Biological Survey: Columbus, OH, USA, 1997; pp. 7–13.
71. Meyer, J.L.; Wallace, J.B. Lost linkages and lotic ecology: Rediscovering small streams. In *Ecology: Achievement and Challenge*; Press, M.C., Huntly, N.J., Levin, S., Eds.; Blackwell Scientific: London, UK, 2001; pp. 295–317.
72. Abdulrazzak, M.J.; Morel-Seytoux, H.J. Recharge from an ephemeral stream following wetting front arrival to water table. *Water Resour. Res.* **1983**, *19*, 194–200. [CrossRef]
73. Camarasa-Belmonte, A.M.; Segura-Beltrán, F. Flood events in Mediterranean ephemeral streams (ramblas) in Valencia region, Spain. *Catena* **2001**, *45*, 229–249. [CrossRef]
74. Poff, N.L.; Allan, J.D.; Bain, M.B.; Karr, J.R.; Prestegaard, K.L.; Richter, B.D.; Sparks, R.E.; Stromberg, J.C. The natural flow regime: A paradigm for river conservation and restoration. *BioScience* **1997**, *47*, 769–784. [CrossRef]
75. Paul, M.J.; Coffey, R.; Stamp, J.; Johnson, T. A review of water quality responses to air temperature and precipitation changes 1: Flow, water temperature, saltwater intrusion. *J. Am. Water Resour. Assoc.* **2019**, *55*, 824–843. [CrossRef]
76. Wolman, M.G.; Miller, J.P. Magnitude and frequency of forces in geomorphic processes. *J. Geol.* **1960**, *68*, 54–74. [CrossRef]

77. Dunne, T. Stochastic aspect of the relations between climate, hydrology and landform evolution. *Trans. Jpn. Geomorphol. Union* **1991**, *12*, 1–24.
78. Ziemer, R.R.; Lisle, T.E. *Hydrology*; Chapter 3 in River Ecology and Management; Naiman, R.S., Ed.; Springer: New York, NY, USA, 1998; pp. 143–162.
79. Johnson, S.L. Factors influencing stream temperatures in small streams: Substrate effects and a shading experiment. *Can. J. Fish. Aquat. Sci.* **2004**, *61*, 913–923. [CrossRef]
80. Wang, H.; Yang, Z.; Saito, Y.; Liu, J.P.; Sun, X. Interannual and seasonal variation of the Huanghe (Yellow River) water discharge over the past 50 years: Connections to impacts from ENSO events and dams. *Glob. Planet. Change* **2006**, *50*, 212–225. [CrossRef]
81. Steel, E.A.; Sowder, C.; Peterson, E.E. Spatial and temporal variation of water temperature regimes on the Snoqualmie river network. *J. Am. Water Resour. Assoc.* **2016**, *52*, 769–787. [CrossRef]
82. Lee, S.; Klein, A.; Over, T. Effects of the El Nino~–southern oscillation on temperature, precipitation, snow water equivalent and resulting streamflow in the Upper Rio Grande river basin. *Hydrol. Process.* **2004**, *18*, 1053–1071. [CrossRef]
83. Novikmec, M.; Svitok, M.; Kočický, D.; Šporka, F.; Bitušík, P. Surface water temperature and ice cover of Tatra mountains lakes depend on altitude, topographic shading, and bathymetry. *Arct. Antarct. Alp. Res.* **2013**, *45*, 77–87. [CrossRef]
84. Pletterbauer, F.; Melcher, A.; Graf, W. Climate change impacts in riverine ecosystem. *Riverine Ecosyst. Manag.* **2018**, *8*, 203–223.
85. Oware, E.K.; Peterson, E.W. Storm driven seasonal variation in the thermal response of the streambed water of a low-gradient stream. *Water* **2020**, *12*, 2498. [CrossRef]
86. Hewlett, J.D.; Hibbert, A.R. Factors affecting the response of small watersheds to precipitation in humid regions. In *Forest Hydrology*; Sopper, W.E., Lull, H.W., Eds.; Pergamon Press: Oxford, UK, 1967; pp. 275–290.
87. Sidle, R.C.; Tsuboyama, Y.; Noguchi, S.; Hosoda, I.; Fujieda, M.; Shimizu, T. Streamflow generation in steep headwaters: A linked hydro-geomorphic paradigm. *Hydrol. Process.* **2000**, *14*, 369–385. [CrossRef]
88. Fekete, B.M.; Vörösmarty, C.J.; Roads, J.O.; Willmott, C.J. Uncertainties in precipitation and their impacts on runoff estimates. *J. Clim.* **2004**, *17*, 294–304. [CrossRef]
89. Voisin, N.; Wood, A.W.; Lettenmaier, D.P. Evaluation of precipitation products for global hydrological prediction. *J. Hydrometeorol.* **2008**, *9*, 388–407. [CrossRef]
90. Biemans, H.; Hutjes, R.W.A.; Kabat, P.; Strengers, B.J.; Gerten, D.; Rost, S. Effects of precipitation uncertainty on discharge calculations for main river basins. *J. Hydrometeorol.* **2009**, *10*, 1011–1025. [CrossRef]
91. Burrel, B.C.; Davar, K.; Hughes, R. A review of flood management considering the impacts of climate change. *Water Int.* **2007**, *32*, 342–359. [CrossRef]
92. Hynes, H.B.N. The stream and its valley. *Proc. Int. Assoc. Theor. Appl. Limnol.* **1975**, *19*, 1–15. [CrossRef]
93. Vannote, R.L.; Minshall, W.G.; Cummins, K.W.; Sedell, J.R.; Cushing, C.E. The river continuum concept. *Can. J. Fish. Aquat. Sci.* **1980**, *37*, 130–137. [CrossRef]
94. Sidle, R.C.; Pearce, A.J.; O'Loughin, C.L. *Hillslope Stability and Landuse*; American Geophysical Union: Washington, DC, USA, 1985; p. 40.
95. Dieterich, M.; Anderson, N.H. The invertebrate fauna of summer-dry streams in western Oregon. *Archiv Hydrobiol.* **2000**, *147*, 273–295. [CrossRef]
96. Benda, L.; Dunne, T. Stochastic forcing of sediment routing and storage in channel networks. *Water Resour. Res.* **1997**, *33*, 2865–2880. [CrossRef]
97. Rice, S.P.; Greenwood, M.T.; Joyce, C.B. Tributaries, sediment sources, and longitudinal organization of macroinvertebrate fauna along river systems. *Can. J. Fish. Aquat. Sci.* **2001**, *58*, 824–840. [CrossRef]
98. Detty, J.M.; McGuire, K.J. Threshold changes in storm runoff generation at a till-mantled headwater catchment. *Water Resour. Res.* **2010**, *46*, W07525. [CrossRef]